# Chain Flips in Polyethylene Crystallites and Fibers Characterized by Dipolar $^{13}C$ NMR§

**W.-G. Hu,† C. Boeffel,‡ and K. Schmidt-Rohr*,†**

*Department of Polymer Science and Engineering, University of Massachusetts, Amherst, Massachusetts 01003, and Max-Planck-Institut für Polymerforschung, D-55021 Mainz, Germany*

*Received July 17, 1998; Revised Manuscript Received December 8, 1998*

ABSTRACT: The occurrence and rate of 180° chain-flip motions in the crystalline regions of two polyethylenes were studied by $^{13}C$ NMR. In high-density polyethylene (HDPE) and in ultradrawn ultrahigh molecular weight polyethylene (UHMWPE) fibers, the changes in the $^{13}C-^{13}C$ dipolar couplings brought about by the reorientations of the $^{13}C-^{13}C$ internuclear vectors in the crystallites were observed. In the HDPE sample, which was labeled with 4% of $^{13}C-^{13}C$ pairs, the rotational motion was observed directly via two-dimensional exchange spectroscopy, stimulated-echo decays, and 1D line shape changes monitoring the $^{13}C-^{13}C$ dipolar coupling. The data show that the jumps occur between two sites, with a rotation angle of 180° and with a jump rate of ∼10/s at ambient temperature**.** The correlation function of the motion was found to be slightly nonexponential, with a stretched-exponential $\beta$ parameter of $0.8 \pm 0.1$. The data yield an activation energy of $93 \pm 10$ kJ/mol for the 180° chain flips. In the fibers, the narrowing of natural-abundance $^{13}C-^{13}C$ dipolar satellites is a clear NMR signature of the chain motion, indicating a jump rate of 150/s at 360 K, which is 20 times slower than in the unoriented HDPE. The correlation time dependence of the $^1H$ $T_{1\rho}$ relaxation time, which probes the modulation of H−H dipolar couplings in the crystallites, was determined directly. Relations between the chain flip motion, the dynamic-mechanical α-relaxation, creep, and drawability are discussed.

## 1. Introduction

The α-relaxation in semicrystalline polymers[1] is related to important materials properties such as creep,[2] annealing,[3] crystallization,[4] extrudability,[5] and drawability.[6] The underlying microscopic chain motions in the crystallites[7] have been elucidated by solid-state NMR in various semicrystalline polymers, including poly(oxymethylene),[8−10] isotactic polypropylene,[9−11] and poly(ethylene oxide).[10] Helical jumps, which are surprising large-amplitude chain rotations, requiring concomitant translations by full chemical repeat units, are directly detected by two-dimensional exchange NMR[10] in terms of changes of the angle-dependent $^{13}C$ chemical shift or $^2H$ quadrupolar coupling. In poly(tetrafluoroethylene),[12,13] translational disorder and in poly(vinylidene fluoride),[14] *trans*-polybutadiene,[15] and possibly in form II of isotactic poly(1-butene)[16] dynamic conformational disorder of similarly large amplitudes have been observed.

In polyethylene, 180° chain flips have long been considered as the dominant mode of the α-relaxation in the crystalline regions.[7,17−20] However, to date these flips have not been observed directly, since the most accessible NMR interactions are invariant under the 180° flip. Chemical shift, geminal H−H dipolar, C−H dipolar,[18] and $^2H$ quadrupolar tensors[21] are exactly inverted by the chain flip, which therefore leaves the corresponding NMR frequencies unchanged. In NMR, the α-relaxation has been studied by observing that the spin−lattice relaxation time in the rotating frame ($T_{1\rho}$), which reflects the modulation of long-range H−H couplings, strongly decreases with increasing temperature for segments in the crystallites.[22] However, most of the available NMR data do not strictly exclude other possible explanations for the α-relaxation in PE. For instance, straight displacement of the chain without rotation would account for most of the available NMR data, including chain diffusion.[23] The $^{13}C-^{13}C$ satellite narrowing observed by VanderHart[24] in oriented PE is the only good NMR indication of chain rotation in PE. Dielectric relaxation observes reorientation of C═O defects in the chains, with a strong direction dependence in oriented samples, which indicates chain rotation in the crystallites.[25] However, most of the defects may be located near the interface, and rotations of limited amplitude around the chain axis might also account for the dielectric data. Recently, NMR line broadening has been interpreted as evidence that more than half of the chains in the crystallites of various high- and low-density polyethylenes undergo 180° flips in the kilohertz range at ambient temperature.[26] Quantitative interpretation of NMR, dielectric, and dynamic-mechanical relaxation measurements is not straightforward and model dependent.

In this work, we present direct observation of the 180° flips in terms of the reorientation of $^{13}C-^{13}C$ internuclear vectors in the crystallites of PE. As indicated in Figure 1a, these C−C bonds reorient by the large bond angle of ∼112°, observed in terms of changes of the $^{13}C-^{13}C$ dipolar couplings in a specially prepared HDPE containing $^{13}C-^{13}C$ spin pairs. The correlation function of the chain reorientation is measured directly in terms of the mixing time dependence of stimulated echoes of the dipolar coupling. Combining these measurements with the analysis of line-shape changes at higher temperatures, the activation energy of the motional process is obtained.

We also report the occurrence of chain flips in highly drawn ultrahigh-molecular-weight polyethylene (UHMWPE) fibers. These are engineering fibers with excel-

† University of Massachusetts.
‡ Max-Planck-Institut für Polymerforschung.
* To whom correspondence should be addressed.
§ For corrections to this paper, see: *Macromolecules* **1999**, *32*, 1714.

10.1021/ma981138t CCC: $18.00 
Published on Web 01/20/1999

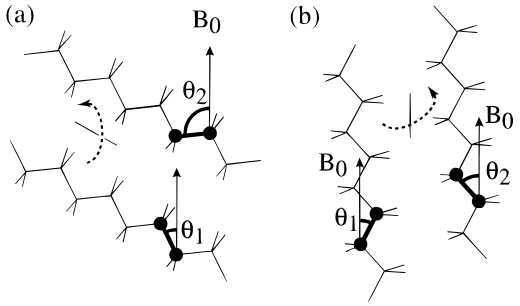


**Figure 1.** Effects of 180° chain flips on $^{13}C-^{13}C$ bonds in polyethylene. The external field $B_0$ is along the vertical direction. (a) General case of a 180° flip in an unoriented sample, producing a great change in the $^{13}C-^{13}C$ bond orientation, from $\theta_1$ to $\theta_2$. Consequently, the orientation-dependent frequency $\omega(\theta)$ will also be changed drastically. (b) Effect of a chain flip in a chain in a slightly misaligned fiber that is part of a fiber bundle oriented along the external field $B_0$. The average of $\theta_1$ and $\theta_2$ will be similar for different degrees of slight misalignment.

lent mechanical properties,[27] which can be produced by tensile drawing of solid-state extruded reactor powder to a final draw ratio of >80. These fibers are ca. 90% crystalline[28,29] and believed to contain continuous crystals over micrometer length scales.[30] This makes it doubtful whether chain flips, which require mobility and "slack" of chains in the amorphous regions, are possible. On the other hand, under large stress, the applicability of the fibers is limited mostly by creep,[31] which is related to the dynamic-mechanical α-relaxation in the crystalline regions.[32] Dielectric studies of the unoxidized and unchlorinated fibers would be challenging. It is our goal to elucidate by NMR whether and how the microscopic chain flips occur in the highly crystalline fibers. When the fibers are aligned with the magnetic field ($B_0$) direction, dynamics of the $^{13}C-^{13}C$ bond can be observed in terms of the narrowing of the dipolar satellites produced by natural abundance $^{13}C$ spin pairs.[24] The relation of the microscopic dynamics and the macroscopic mechanical behavior such as creep and the dynamic-mechanical relaxation will be discussed.

## 2. Experimental Section

**Samples.** The melt-crystallized high-density polyethylene labeled with dilute $^{13}C-^{13}C$ spin pairs was prepared by copolymerizing ~95% natural abundance and ~5% doubly $^{13}C$-labeled ethylene, using a titanium catalyst. A 100 mg (3.4 mmol) sample of $^{13}C$-labeled ethylene was transferred into an evacuated 2 L flask containing the catalyst in toluene, and then the remaining volume was quickly filled to atmospheric pressure with 85 mmol of unlabeled ethylene gas. The flask was sealed and then stirred for 24 h, producing a slurry of the polymer and catalyst in toluene which was poured into an excess of isopropyl alcohol.

The actual ratio of directly bonded and isolated $^{13}C$ nuclei was determined to be close to 4.4:1.1 in the analysis of the experimental $^{13}C$ spectra shown below. The sample was melted in a glass tube with 4 mm i.d. and cooled in air. Two heating cycles (up to 360 K for 2 h) were applied before the variable temperature $T_{1\rho,H}$ measurements. The sample before and after this thermal treatment is termed HDPE-b and HDPE-a, respectively. A commercial random copolymer of ethylene and hexene, produced by a Ziegler−Natta catalysts, was used to measure the minimum value of $T_{1\rho,H}$. The mole fraction of hexene in the sample was 4.4%.

The ultradrawn UHMWPE polyethylene fibers (in a tape of a cross section of 0.1 mm × 1.8 mm) were kindly provided by the late Prof. R. S. Porter. The molecular weight (viscosity average) is about $4 \times 10^6$. To produce the fibers, films of compacted Himont Hifax 1900 reactor powder were solid state extruded at 110 °C to a draw ratio of 5, followed by tensile drawing at 135 °C resulting in a fibrous tape. The final draw ratio achieved is 82−85, with a tensile modulus of up to 130 GPa. No isotope labeling was used. A uniaxially oriented sample for the NMR experiments was produced by aligning many layers of the tape parallel to each other and wrapping the bundle with Teflon tape, which is invisible in $^1H-^{13}C$ cross-polarization experiments. Two sections of 6 mm length were cut out and aligned in the NMR radio-frequency coil of 8 mm diameter. The NMR spectra show that the fibers in the bundle are on average parallel within ±4°.

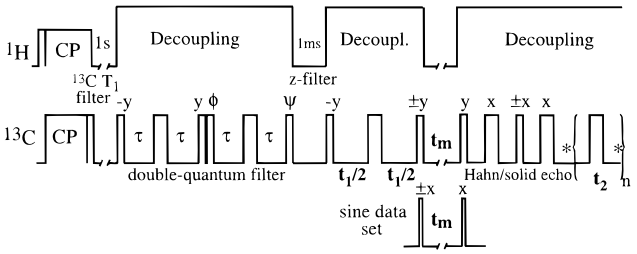


**Figure 2.** 2D pulse sequence to detect reorientations of $^{13}C-^{13}C$ dipolar tensors. After a $T_1$ filter to suppress the amorphous-phase signal, a double-quantum filter removes the signal of isolated $^{13}C$ spins (with $\phi = x, y, -x, -y$ and $\psi = x, -y, -x, y$). During the evolution time $t_1$, a single 180° pulse refocuses the chemical shift, retaining the pure $^{13}C-^{13}C$ dipolar coupling. During the long mixing time $t_m$, segmental reorientations may occur, which are detected in terms of the changed $^{13}C-^{13}C$ dipolar frequency. A Hahn−solid−Hahn echo[34] before detection allows for dead-time-free detection. During $t_2$, a train of 180° pulses with phases [α, α, −α, −α] perpendicular to the initial magnetization constantly refocuses the chemical shift while data points are acquired at the times denoted by "*". The sequence shown in the middle, with 90° pulses flanking the mixing time $t_m$, produces the cosine data set, while the 45° pulses indicated at the bottom yield the sine data set (see text).

**NMR Experiments.** The NMR experiments were performed on a Bruker MSL-300 spectrometer at a $^{13}C$ frequency of 75.48 MHz and a $^1H$ frequency of 300.13 MHz. Various NMR techniques were used to obtain a more comprehensive understanding of the material:

1. $^{13}C-^{13}C$ dipolar coupling 2D exchange experiment. As in the related 2D dipolar DECODER experiment by Utz et al.,[33] the pure C−C dipolar coupling was detected in both dimensions. An illustration of the pulse sequence is shown in Figure 2, with the main trace shown for the cosine data set. For the sine data set, the two 90° pulses before and after $t_m$ are replaced by $45°_x$ and $45°_{-x}$, respectively, as shown at the bottom of the figure. A double-quantum filter before the 2D exchange sequence was used to remove the contribution from isolated $^{13}C$ sites, which otherwise produces a very high peak in the center of the spectrum, with concomitant baseline distortions. To minimize the nonuniform excitation effect from the double-quantum filter, data with double-quantum excitation/reconversion times of 140, 280, 420, 560, 700, and 840 μs were added up. Before the start of detection, the dead-time problem was overcome by a Hahn−solid−Hahn echo which refocuses both the chemical shift and the $^{13}C-^{13}C$ dipolar coupling.[34] The experiment was performed at ambient temperature. The mixing time was 100 ms. The signal of the amorphous regions was suppressed by a $T_{1,C}$ filter of 0.4 s. A total of 48 data points were acquired in the first dimension, for both sine and cosine data sets, with an increment of 48 μs. The $^1H$ decoupling field strength was $(\gamma B_1/2\pi) > 120$ kHz in a coil of 5 mm diameter.

2. Stimulated echo decay measurement,[10,35] using the pulse sequence of Figure 2 (cosine data set) with $t_2 = t_1 = 1.25$ ms. The intensity of the $^{13}C-^{13}C$ dipolar stimulated echo produced at $t_2 = t_1$ was measured as a function of the mixing time $t_m$. A $T_{1,C}$ filter of 1.5 s and a double-quantum filter were applied to remove the signal contributions of the amorphous phase and isolated $^{13}C$ sites. The recycle delay was 3 s.

3. 1D $^{13}C$ line shape of the crystalline regions at various temperatures. A $T_{1,C}$ filter of 1.5−3 s was applied to remove the signal of the amorphous regions. It reduces the signal of the all-trans segments by less than 10%. The recycle delay was 3−4 s. Longer filter and recycle delays were used at higher temperatures. The decoupling field strength was >120 kHz. Before detection, a Hahn−solid−Hahn echo[34] with a total preecho delay of 90 $\mu$s was applied at 310 K and below. A Hahn spin echo with a total preecho delay of 32 $\mu$s was used at higher temperatures.

4. Narrowing of the $^{13}C-^{13}C$ dipolar satellites at elevated temperature (360 K) in UHMWPE fibers aligned along the $B_0$ field. The pulse sequence was cross polarization (CP) with $^1H$-decoupled $^{13}C$ detection. The decoupling field strength ($\gamma B_1/2\pi$) was 55 kHz. For each spectrum, approximately 20 000 scans were averaged, with a recycle delay of 7 s.

5. Crystalline $T_{1\rho,H}$ at various temperatures and sample orientations with respect to the $B_0$ field. The spin-lock field ($\gamma B_1/2\pi$) was 55 kHz. The pulse sequence consisted of a variable $^1H$ spin-lock, cross-polarization to $^{13}C$, a 0.6 s phase-cycled z-filter to suppress the signal of the noncrystalline regions based on their short $T_{1,C}$, and $^1H$-decoupled $^{13}C$ detection. The cross-polarization time was 0.1 ms. Hardware consideration limited the radio-frequency irradiation for the spin-lock to less than 30 ms.

## 3. NMR Techniques and Results

In the following sections, the principles and results of the various NMR techniques applied to $^{13}C-^{13}C$ labeled HDPE and unlabeled UHMWPE fibers will be presented.

**2D Exchange Spectrum.** As an alternative to the treatment in ref 33 where a similar experiment, but with sample flip in the mixing time, was applied to polycarbonate, we describe the evolution of the density operator in terms of simple Cartesian product operators. In the following derivations, $S$ and $L$ stand for two directly bonded $^{13}C$ nuclear spins. We consider the strong-coupling limit of the homonuclear dipolar coupling, where the difference of the chemical shift frequencies between $S$ and $L$ is always zero, as appropriate for the all-trans conformation of crystalline polyethylene. Using Pauli matrices to represent the spin operators of the spin-$^1/_2$ nuclei,[10] one obtains the following simple dipolar evolution

$$\rho(t) = (S_x + L_x)\cos(\omega_{d,1}t_1) + 2(S_yL_z + S_zL_y)\sin(\omega_{d,1}t_1) \quad (1)$$

where the dipolar coupling frequency is

$$\omega_{d,1} = -\frac{3}{2}\frac{\mu_0}{4\pi}\hbar\frac{\gamma^2}{r_{CC}^3}\frac{1}{2}(3\cos^2(\theta_1) - 1)$$

$\theta_1$ is the angle between the magnetic field and the C−C bond before the mixing time, and $r_{CC}$ is the distance between the two $^{13}C$ nuclei. To obtain spectra with the maximum possible quadrature information, two data sets were combined. As indicated in Figure 2, the "cosine" data set is obtained from the cosine-modulated magnetization by the standard phase cycle of $\pm z$ storage, 90° readout pulse of phase $\alpha$, and $\pm(\alpha + 90°)$ detection phases, which yields a signal $\langle\cos(\omega_{d,1}t_1)\cos(\omega_{d,2}t_2)\rangle$.

The sine data sets require more careful consideration. The necessary modification of the pulse sequence is shown at the bottom of Figure 2. By a $45°_{-x}$ storage pulse at the end of the $t_1$ period, the density operator is converted to

$$(S_x + L_x)\cos(\omega_{d,1}t_1) + 2\left[\frac{1}{\sqrt{2}}(S_y + S_z)\frac{1}{\sqrt{2}}(L_z - L_y) + \frac{1}{\sqrt{2}}(S_z - S_y)\frac{1}{\sqrt{2}}(L_y + L_z)\right]\sin(\omega_{d,1}t_1) \quad (2)$$

of which $2S_zL_z\sin(\omega_{d,1}t_1)$ survives after $T_2$ relaxation of the transverse terms. By a $45°_x$ readout pulse, this is converted to $2(1/\sqrt{2}S_z + 1/\sqrt{2}S_y)(1/\sqrt{2}L_z + 1/\sqrt{2}L_y)\sin(\omega_{d,1}t_1)$, of which $(S_zL_y + S_yL_z)\sin(\omega_{d,1}t_1)$ becomes observable magnetization under the action of the dipolar coupling, according to

$$(S_zL_y + S_yL_z)\sin\omega_{d,1}t_1 \rightarrow (S_zL_y + S_yL_z)\sin(\omega_{d,1}t_1)\cos(\omega_{d,2}t_2) - {}^1/_2(S_x + L_x)\sin(\omega_{d,1}t_1)\sin(\omega_{d,2}t_2) \quad (3)$$

The observed signal is thus $^1/_2\langle\sin(\omega_{d,1}t_1)\sin(\omega_{d,2}t_2)\rangle$. The factor of $^1/_2$ must be compensated by scaling the sine data set up by a factor of 2. Acquiring the sine data with twice the number of scans relative to the cosine data set is a convenient alternative that yields a slightly better signal-to-noise ratio per unit time. This approach was adopted here. The data were measured and combined in $t_1$ according to the TPPI scheme and processed accordingly on the MSL spectrometer. To remove residual signal along the antidiagonal which may be due to pulse imperfections, the sine data set was scaled by a factor of 1.1 before combination with the cosine data set. The experiment was performed on sample HDPE-b, and the spectrum shown in Figure 3a was obtained in 2 days of signal averaging. It exhibits intensity far from the diagonal, which indicates large changes in frequency and orientation due to the motion in the 100 ms mixing time. The elliptical ridges observed in the spectral intensity patterns are well-known from $^2H$ exchange NMR.[10,36] They have an ratio of half-axis lengths of $b/a = 2.5 \pm 0.5$. According to $|\tan\beta| = b/a$,[3,6,10] this yields a reorientation angle $\beta$ of $112 \pm 5°$ or $68 \pm 5°$.

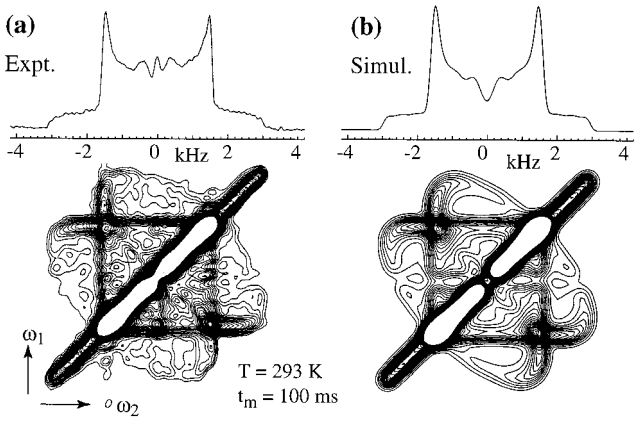


**Figure 3.** 2D exchange spectrum of the $^{13}C-^{13}C$ dipolar coupling in $^{13}C-^{13}C$ pair labeled HDPE. (a) Experimental spectrum, $T$ = 293 K, $t_m$ = 100 ms. (b) Corresponding simulation for 180° flips. Thirty contour lines are plotted between 0.8% and 20% of the maximum intensity. The slight asymmetry of the spectrum is due to the double-quantum filter, which does not excite equally the signals for all $^{13}C-^{13}C$ orientations. Integral projections onto the $\omega_2$ axis are shown at the top.

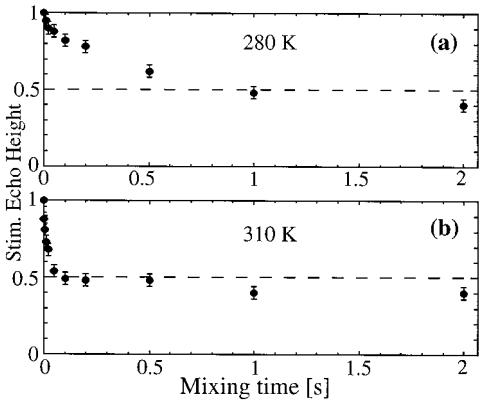


**Figure 4.** $^{13}C-^{13}C$ dipolar stimulated echo height as a function of mixing time at (a) 280 K and (b) 310 K. At $t_m < 0.5$ s, the decay is due to reorientations of the $^{13}C-^{13}C$ vectors; at $t_m > 0.5$ s, there is a significant effect of spin diffusion between chains of different orientation.

A simulation of the above exchange experiment is shown in Figure 3b. It is based on a reorientation of the C−C bond by $\beta = 112°$ before and after the 180° rotation around the chain axis. A C−C bond length of 1.56 ± 0.01 Å and a C−C−C bond angle of 112 ± 2° were used in the simulation.[37] Spectra with different double-quantum evolution times, as described in section 2, were added up. The experimental and simulated spectra are slightly asymmetric due to the double-quantum filtering. The jump rate used in the simulation was 15/s, which was determined by a stimulated echo measurement applied to the same sample (HDPE-b) at the same temperature.

**Dipolar Coupling Stimulated Echo Experiments.** The intensity of the stimulated echo[10,35] generated by the $^{13}C-^{13}C$ dipolar coupling was recorded as a function of the mixing time to measure the correlation function of the 180° flip motion. The stimulated echo is due to the $^{13}C$ sites that have the same frequency before and after the mixing time. For a two-site jump process such as the 180° flip motion, ideally the echo height after complete loss of correlation after long mixing time is one-half of the original value at short $t_m$. Actually, spin diffusion between $^{13}C$ nuclei on different chains further reduces the echo height at long mixing time. This restricts the correlation time measurements at low temperatures. The limitation at high temperatures is the requirement of the slow-motion regime ($\tau_c > 2t_1$), which means that during the dephasing period $t_1$ and refocusing period $t_2 = t_1$ no reorientation of the $^{13}C-^{13}C$ pair occurs. Therefore, we limited our measurement to temperatures ≤310 K ($\tau_c > 20$ ms).

Figure 4 shows the echo height decay as a function of the mixing time at 280 and 310 K. At 310 K, a constant value of $\sim 1/2$ is observed between 0.1 and 0.5 s. At $t_m \geq 1$ s, the echo height decays to $< 1/2$ due to spin diffusion. At 280 K, where the motion is slower, the echo decay due to reorientation and spin diffusion occurs on similar time scales.

Figure 5a shows the correlation function in sample HDPE-a at various temperatures as a function of reduced mixing time, $t_m/\tau_c$, where $\tau_c$ is obtained by best fit with a single-exponential function. The fit with a stretched exponential $\exp(-(t_m/\tau_c)^\beta)$ for $\beta = 0.8 \pm 0.1$ is shown in Figure 5b; here, $\tau_c$ is obtained by best fit with the stretched-exponential function. The stretched exponential is found to fit the experimental data significantly better.

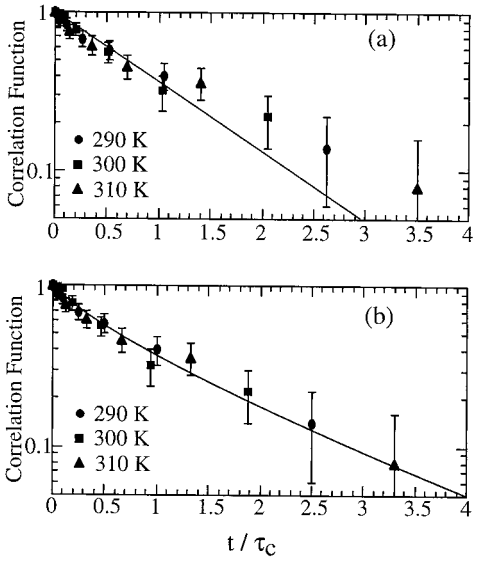


**Figure 5.** Correlation function from stimulated-echo decays vs reduced mixing time $t/\tau_c$ at 290, 300, and 310 K, with (a) single-exponential fit and (b) stretched-exponential $\exp(-(t/\tau_c)^{0.8})$ fit.

**Motional Rates from $^{13}C$ Line Shape Changes.** The 1D line shape reflecting $^{13}C-^{13}C$ dipolar coupling and chemical shift depends on the motional rate, which can be quantified by comparison with simulated spectra. According to Abragam,[38] the line shape of a single segment that undergoes jumps between two sites with average frequency $\bar{\omega}$ and splitting $2\delta$ is given by

$$I(\omega) \propto \frac{4\delta^2 k}{(\omega - \bar{\omega})^4 + 2(\omega - \bar{\omega})^2(2k^2 - \delta^2) + \delta^4} \quad (4)$$

where $k$ is the flip rate, $k = 1/(2\tau_c)$. For $k \ll \delta$ (slow limit), two sharp lines at $\omega = \bar{\omega} \pm \delta$ are observed. For $k \gg \delta$ (fast limit), only one sharp line at $\omega = \bar{\omega}$ is observed due to motional averaging.

In the case of interest here, the frequencies $\bar{\omega} + \delta$ and $\bar{\omega} - \delta$ are produced by the simultaneous action of $^{13}C-^{13}C$ dipolar couplings and $^{13}C$ chemical shift anisotropies. For a flip between two given $^{13}CH_2-^{13}CH_2$ segment orientations, the average frequency $\bar{\omega}$ depends on both the (invariant) chemical shift anisotropy and the average dipolar coupling, while the splitting $\delta$ reflects the difference between the dipolar couplings for the two $^{13}C-^{13}C$ vector orientations. The calculation is performed most conveniently in the principal axes system of the $^{13}CH_2$ chemical shift tensor.[39] Here, the orientations of the $^{13}C-^{13}C$ internuclear vectors before and after the flip are fixed and well-defined, so that the dipolar frequencies can be calculated easily from the angle between the $B_0$ field and the $^{13}C-^{13}C$ internuclear vector.[10] The powder spectrum is obtained by summing up spectra calculated according to eq 4 for all orientations of the $B_0$ field, with the polar coordinates ($\beta$, $\alpha$) incremented by 0.5° and 1°, respectively. The parameters used in the simulations are as follows: a bond length and a bond angle of 1.56 Å and 112°, respectively, as in the 2D exchange simulations;[37] chemical shift principal values of 50, 35, and 13 ppm;[40] $^{13}C-^{13}C$ spin pairs and isolated $^{13}C$ population in a ratio of 4:1.

Figure 6a shows the 1D spectra of HDPE-a at various temperatures. The line shape changes at elevated temperatures as a result of the chain motion. Figure 6b shows the corresponding simulations based on 180°

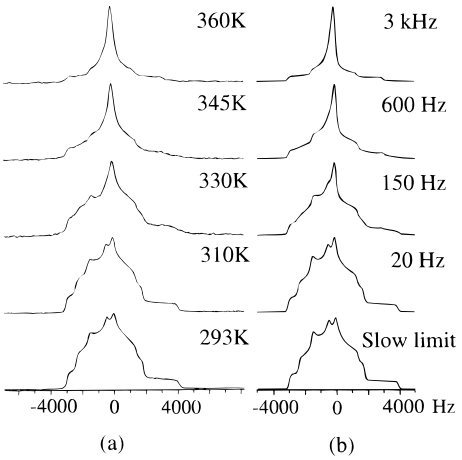


**Figure 6.** 1D $^{13}C$ NMR line shapes of the crystalline regions, reflecting dipolar coupling and chemical shift. (a) Experimental spectra as a function of temperature. (b) Corresponding simulations, with the indicated jump rates.

flip motion, in which the chemical shift is invariant while $^{13}C-^{13}C$ dipolar coupling tensor changes. As seen from the figure, the motion can be well described by this flip motion. The determination of the flip rate from the one-dimensional line shape is reliable in a window of rates between 10/s and $10^4$/s. Outside the window, the system is in the fast- or slow-motion limit, and the line shape is not sensitive to the motional rate.

**Flip Rates in UHMWPE Fibers from Narrowing of Dipolar Satellites.** Studying the motion in unenriched PE by reorientation of $^{13}C-^{13}C$ pairs is much more difficult because these spin pairs represent only an extremely small fraction (2.2/10000) of all carbon sites. Still, in highly oriented polyethylene fibers aligned with the $B_0$ field, the $^{13}C-^{13}C$ spin pairs produce observable dipolar satellites.[24] A slight distribution in chain orientations leads to a broadening of the satellite. If the motional rate exceeds the width of the satellite, it narrows because the average dipolar frequencies for slightly misaligned chains are all similar; see Figure 1b.

Various arrangements of $^{13}C$ nuclei occur statistically and can be distinguished based on their $^{13}C-^{13}C$ dipolar couplings: (a) isolated $^{13}C$ sites (C), (b) directly bonded $^{13}C$ pairs ($R_1$), and (c) $^{13}C$ pairs ($^{13}C-C-^{13}C$) separated by two bonds ($R_2$). The spectrum of site C reflects only the chemical shift, while sites $R_1$ and $R_2$ experience a chemical shift as well as different dipolar couplings. When the fiber axis is aligned parallel to $B_0$, the resonance frequency of site C does not have a strong angle dependence because one of the principal axes of the chemical shift tensor is parallel to $B_0$. The angle dependence of the $R_2$ dipolar coupling is $\omega(\theta) = -2\pi\cdot 620$ Hz $\times$ $(3\cos^2\theta - 1)/2$, where $\theta$ is the angle between the internuclear $^{13}C-^{13}C$ vector and the $B_0$ field. For $R_2$, $\theta \approx 0$ and the angle dependence of the frequency is small due to $d\omega/d\theta|_0 = 0$. On the other hand, the dipolar coupling of the $R_1$ pair, which is $\omega(\theta) = -2\pi\cdot 3$ kHz $\times$ $(3\cos^2\theta - 1)/2$ with an average $\theta$ angle of 34°, has a strong angle dependence, $d\omega/d\theta|_{34} = 2\pi\cdot 70$ Hz/deg. Since the chain axes are not perfectly aligned along the magnetic field, in the absence of significant chain motion the $R_1$ peak is much broader than those of C and $R_2$.

As proven for unoriented HDPE above, the crystalline chain motion in PE is a 180° chain-flip motion during which the chain flips by 180° and translates by one $CH_2$ unit so that the chain after the flip still fits the crystal lattice. In oriented PE, the flip motion leaves the $^{13}C$ chemical shift tensor invariant, but the $R_1$ dipolar coupling changes before and after the flip for chains that are not perfectly aligned along $B_0$ (see Figure 1b).[24] Thus, the 180° flip motion in the crystalline region will cause motional averaging of the $R_1$ signal due to the $^{13}C-^{13}C$ bond reorientation. As a result, if the motional rate is high enough, i.e., comparable to the low-temperature line width of the $R_1$ peaks, we will see narrowing of the $R_1$ satellites.

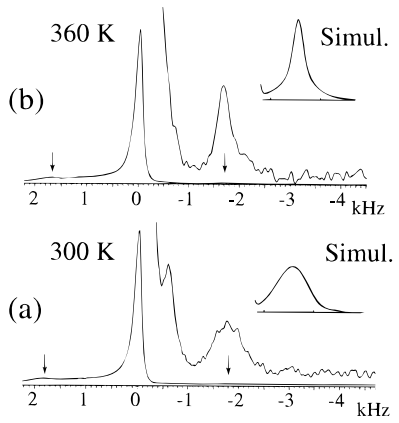


**Figure 7.** $^{13}C$ spectra of UHMWPE fibers with fiber axes parallel to $B_0$, demonstrating motional narrowing of a $^{13}C-^{13}C$ dipolar satellite. The positions of the satellites are indicated by the two vertical arrows. (a) Experimental spectrum at room temperature (~300 K) and simulation (inset) of the dipolar satellite for a flip rate of $k < 10$/s. The upper trace of the experimental spectrum was expanded vertically by a factor of 128; 100 Hz line broadening was applied. (b) Experimental spectrum at 360 K and simulation (inset) for a flip rate of $k = 150$/s. Narrowing of the dipolar satellite is observed clearly.

Figure 7a shows the room-temperature spectrum with two different vertical scales, as well as corresponding simulations. The high and sharp central peak at 13 ppm is due to isolated $^{13}C$ spins. The broad and small peak ($R_1$), at ~1790 Hz from the central peak, is one of the two dipolar satellites (indicated by arrows in the figure) of the directly bonded $^{13}C-^{13}C$ pairs. The dipolar satellite at about 590 Hz from the central peak is generated by $^{13}C-C-^{13}C$ pairs ($R_2$). The full widths at half-height of the central and $R_1$ peaks are 160 and 650 Hz, respectively. The $R_2$ peak overlaps with the tail of the central peak, but it can be seen that it is sharper than the $R_1$ peak. From the single-site signal shape it is clear that, besides a major highly oriented component (~80%) that contributes to the narrow part of the peak, there is a considerable amount of less oriented segments in the sample (~20%) that contribute to the low and wide shoulder on the left.

Simulations were performed to fit the $R_1$ peak at room temperature and at 360 K. The orientation distribution used in the simulation was composed of two parts with Gaussian angular distributions: $\sigma = 4°$ (80%) and 23° (20%). Parameters used in the simulation are the C−C bond length of 1.56 Å and the C−C−C bond angle of 116°.[37] Gaussian line broadening of 100 Hz was applied. The overall order parameter $S_2$ can be estimated from the simulation parameters to be $0.92 \pm 0.02$. Since the CP spectrum underestimates the amorphous phase contribution, the actual $S_2$ should be slightly lower than this value.

The experimental spectrum at 360 K is shown in Figure 7b. The $R_2$ peak is almost invisible due to additional broadening of the central peak. The width

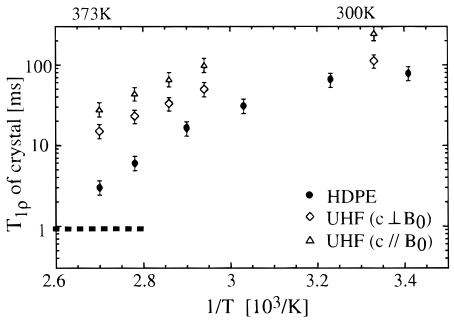


**Figure 8.** $T_{1\rho,H}$ data at various temperatures: (●) HDPE, (◇) UHMWPE fibers with fiber axis perpendicular to $B_0$, (△) fiber axis parallel to $B_0$. The level of the $T_{1\rho,H}$ minimum at 0.9 ms is indicated by the dashed line.

of the $R_1$ peak is ∼350 Hz, showing significant line narrowing compared to the room-temperature width of ∼650 Hz. This demonstrates that 180° flip motion does occur in the highly crystalline UHMWPE fibers. A simulation of the satellite line shape, based on formula 4, is shown as an inset in Figure 7b. It gives a flip rate of 150 ± 50 Hz at 360 K. Significant narrowing was not observed below 340 K. Besides the narrowing, the distance of $R_1$ from the center peak decreases from 1790 Hz at room temperature to 1690 Hz at 360 K, consistent with VanderHart's observation in a different oriented polyethylene.[24]

**Motional Rates and $T_{1\rho,H}$ Relaxation.** The relaxation time $T_{1\rho,H}$ of spin-locked $^1$H magnetization in crystalline PE is sensitive to the chain-flip motion. $T_{1\rho,H}$ detects the modulation of H−H dipolar couplings. It exhibits a minimum when the jump rate $k = 1/(2\tau_c) = \gamma B_1$.[38] In our measurements, $\gamma B_1 = 350$ kHz. Under the 180° chain flips of PE, the strongest dipolar interactions, the geminal H−H dipolar couplings, are invariant. However, the long-range couplings to most other protons do change due to the flip.

Figure 8 shows $T_{1\rho,H}$ of the crystallites in HDPE-a, and in UHMWPE fibers at two different orientations, as a function of temperature. Our measurements cover only the slow-motion regime of $T_{1\rho,H}$, in which $T_{1\rho,H}$ decreases with increasing temperature, toward its minimum of $T_{1\rho\ H,min} \approx 0.9 \pm 0.3$ ms, which was measured on the crystalline $CH_2$ units in the ethylene−hexene copolymer sample at a similar $B_1$ field (indicated by a dashed line). Because of the invariance of the strongest coupling, the depth of the $T_{1\rho,H}$ minimum in PE[22] is less pronounced than, for instance, in the helical jumps of the $7_2$ helix[10] of poly(ethylene oxide).[41]

At low temperatures, the sensitivity of $T_{1\rho,H}$ to the chain flips is compromised by $^1$H spin diffusion to the amorphous regions. Due to the higher mobility, $^1$H magnetization in the amorphous regions relaxes faster. Therefore, these regions act as "sinks" for magnetization in the crystallites, with the coupling between the domains provided by $^1$H spin diffusion. In the UHMWPE fibers, spin diffusion occurs on a time scale of 15 ms,[29] but it should be noted that under the spin lock during the $T_{1\rho}$ measurement, $^1$H−$^1$H dipolar couplings and spin diffusion are reduced by a factor of 0.5. Thus, spin diffusion requires ca. 30 ms of spin lock to affect the magnetization in the crystallites. Even more importantly, the small (∼15%)[29] amorphous and interfacial components in the fibers relax the crystalline regions only very inefficiently on a time scale during which the exchange in a Goldman−Shen experiment is incomplete. Therefore, the crystalline $T_{1\rho}$ of 23 ms ($c||B_0$) at 360 K is reduced little by spin diffusion and reflects the intrinsic relaxation time in the crystallites to a good approximation.

Since relaxation cannot occur faster than the loss of correlation in the underlying dynamic process, for the true rotating-frame relaxation without spin diffusion, $T_{1\rho} > \tau_c$. Thus, we conclude that the motional rate at 360 K must exceed (23 ms)$^{-1}/2 = 20$ Hz. This lower limit is consistent with the flip rate of ∼150 Hz estimated from the satellite narrowing. The combination of intrinsic $T_{1\rho}$ relaxation and spin diffusion at lower temperatures can lead to a complex behavior.[42] However, it is certain that the apparent $T_{1\rho}$ values for the crystallites are shorter than the true ones, since they are partially equilibrated with the shorter $T_{1\rho}$ in the amorphous regions.

It is interesting to note that $T_{1\rho,H}$ of the crystallites in the fiber aligned with $B_0$ is twice as long as that of fibers perpendicular to $B_0$, at all temperatures measured. This shows directly that the relaxation process originates in oriented regions in the sample. A similar effect in the dielectric relaxation in highly oriented extruded polyethylene was taken as evidence that the α-relaxation occurs in the crystallites.[25]

## 4. Discussion

**Geometry of the Chain Motion in the Crystallites.** The two-dimensional exchange NMR spectrum of Figure 3 and the decay of the stimulated echo height to $^1/_2$ in Figure 4b provide the most direct proof available to date for exact 180° jumps in the α-relaxation of polyethylene. The off-diagonal intensity pattern in the 2D spectrum depends sensitively and exclusively on the reorientation angle of the $^{13}$C−$^{13}$C internuclear vector. As required for the 180° rotation of the chain, the reorientation angle matches the C−C−C bond angle of 112°. There is no sign of a significant distribution of reorientation angles; the spectrum is only consistent with a width of less than ±7° around 112°.

While the off-diagonal pattern reflects the reorientation geometry, the relative intensity of off-diagonal and on-diagonal signals yields information on the number of sites involved in the motion and the occupancy of these sites. This information is obtained in a more easily quantifiable manner from the stimulated-echo height, which reflects the fraction of the intensity along the diagonal in the 2D spectrum. The final echo height of $^1/_2$ observed in Figure 4b at 0.1 s < $t_m$ < 0.5 s, i.e., before spin diffusion sets in, shows that at long times the probability of a $^{13}$C−$^{13}$C bond being parallel to its original orientation is $^1/_2$. This confirms the 180° flips, which involve exactly two bond orientations.

Both the well-defined geometry and parallelity of bonds contradict Wunderlich's simulations that predict major disorder in polyethylene crystallites at ∼300 K.[43] $^2$H NMR by Hentschel et al. shows that the C−H bonds in HDPE undergo fast librations with a root-mean-square amplitude of only 4° at 295 K.[21] This is consistent with the observation of little motional averaging of the $^{13}$C−$^{13}$C dipolar couplings in the one-dimensional spectrum obtained at 300 K; see Figure 6, bottom.

**Correlation Function.** The stimulated-echo decay measures the occupancy of $^{13}$C−$^{13}$C bond orientations parallel to the initial orientation, as a function of the mixing time $t_m$. Thus, it maps out the correlation function of the motion. For a jump motion between two

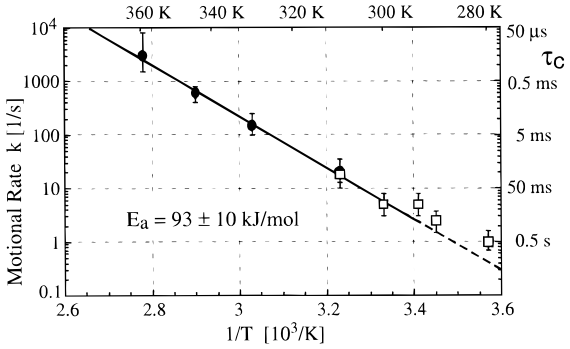


**Figure 9.** Arrhenius plot of the correlation times of the 180° flip motion in the crystallites obtained from the stimulated-echo decays (□) and the 1D line shape changes (●) (see Figure 6). The slope of the line yields an activation energy of 93 ± 10 kJ/mol. Points at the lowest temperatures were excluded from the fit since spin diffusion increases the rate of exchange artificially.

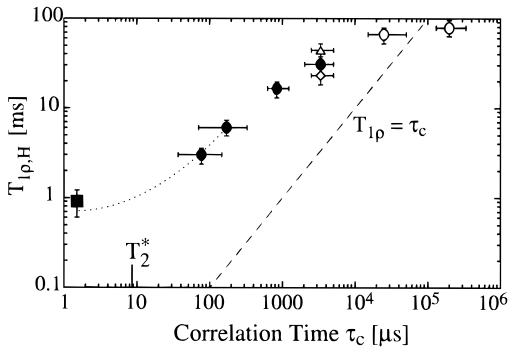


**Figure 10.** Plot of $T_{1\rho,H}$ as a function of correlation time $\tau_c$. Data shown are for HDPE (● in the range little affected by spin diffusion, ○ for $T_{1\rho,H} > 30$ ms), for UHMWPE fibers with fiber axis perpendicular to $B_0$ (◇) and for UHMWPE fibers with fiber axis parallel to $B_0$ (△). The $T_{1\rho}$ minimum at $\tau_c = {}^1/_2\gamma B_1 = 1.4$ $\mu$s (■) was measured on the ethylene−hexene copolymer sample. To indicate that the data will not fall on a straight line because of the minimum, a dotted line with this minimum behavior has been drawn through the data points as a guide to the eye. The dashed line indicates where $\tau_c = T_{1\rho,H}$. The transverse relaxation time $T_2$*, at which the $^1$H FID decays to 1/e, is given on the $\tau_c$ axis. For $T_{1\rho,H} > 30$ ms, effects of spin diffusion become significant. In that range, the $\tau_c$ dependence of $T_{1\rho,H}$ plotted here cannot be expected to be valid for other PE samples.

equally probable bond orientations, this correlation function is given by $p_0(t) = \exp(-t_m/\tau_c)$. The correlation time $\tau_c$ is related to the jump rate $k$ between the two sites according to $\tau_c = 1/(2k)$. The data displayed in Figure 5 show that a stretched exponential $\exp(-(t_m/\tau_c)^\beta)$ with $\beta = 0.8$ gives a significantly better fit than a monoexponential function. This indicates the superposition of correlation functions with different relaxation times. The $\beta$ value of 0.8 corresponds to a width of the relaxation time spectrum of about 0.5 decades,[44] which is close to the result obtained for the dielectric α-relaxation[45] while significantly narrower than that of the dynamic-mechanical α-relaxation.[46]

The decay of the correlation functions to a final value of $^1/_2$ indicates that the chain energies before and after the jump are similar. This is in agreement with 3D exchange NMR observations on POM, where little preference for return jumps was found.[10] A difference could arise due to the change of the length and torsion of the chain segments in the amorphous phase on either end of the chain stem in the crystal.

**Motional Rate of Chain Flips in HDPE.** The temperature dependence of the motional rates of the 180° flip motion, as obtained from the line shape analysis of Figure 6 and from stimulated-echo measurements, is shown in the Arrhenius plot of Figure 9. Data points at $T \geq 290$ K fall on a straight line. The points at the lowest rates and temperatures have higher apparent rates, due to temperature-independent spin diffusion (see Figure 4) which contributes to the stimulated-echo decay. Therefore, they were excluded from the determination of the activation energy. The activation energy of the motion obtained from the slope of the line is $E_a = 93 \pm 10$ kJ/mol. This result is close to dielectric relaxation results of $E_a = 99$ kJ/mol in lightly chlorinated[45] and $E_a = 106$ kJ/mol in lightly oxidized high-density polyethylene.[1,47] For various polyethylenes, values of 100−120 kJ/mol are quoted for the dielectric and dynamic-mechanical crystalline α-relaxations.[7]

Recently, it was proposed that 60−90% of chains in both high- and low-density polyethylenes undergo fast 180° flips in the kilohertz range at ambient temperature.[26] This conclusion was based on a bimodal line shape and cross-polarization inversion of the crystalline signal in magic-angle-spinning (MAS) NMR spectra of various polyethylenes. However, this bimodal line shape is not observed in MAS spectra of similar PEs obtained by other groups.[48] The measurement of $^{13}$C−$^{13}$C bond reorientations in one- and two-dimensional spectra presented in the present work allows for a much more direct observation of the chain dynamics. The spectral line shapes and $T_{1\rho}$ relaxation times shown above contain no signs of fast flipping units at ambient temperature. They directly preclude that more than ∼20% of the crystalline segments in HDPE undergo fast 180° flips at 300 K.

The line shape measurements described in this work depend on motional averaging of orientation-dependent frequencies before and after the 180° flip. Certain other possible motional modes in the crystalline regions such as translation of chain without flipping or 360° rotation with translation would not produce line shape changes but reduce $T_{1\rho,H}$ due to the modulation of the resulting long-range H−H couplings. No indications of such motions are seen here or in chain diffusion measurements,[23] and their calculated activation energies are higher than those for the chain flips.[49]

**Dependence of $T_{1\rho,H}$ on $\tau_c$.** From the $^{13}$C line shape and $T_{1\rho,H}$ measurements on the same sample at various temperatures, a relation between $T_{1\rho,H}$ and the correlation time of the 180° flip motion can be obtained. It is plotted in Figure 10, which can be used as a calibration curve to estimate the 180° flip motion rate in a PE material from its $T_{1\rho,H}$, provided that $T_{1\rho,H} < 30$ ms. Such a curve should prove useful since $T_{1\rho,H}$ can be measured very quickly and easily on any polyethylene sample. The data points for the HDPE and the fiber fall in the same region, which confirms that the same motional rates will lead to similar $T_{1\rho,H}$ for different polyethylene materials. When the motion is too slow ($\tau_c > 50$ ms), we find $T_{1\rho,H} < \tau_c$. Since the relaxation cannot be faster than the underlying motion, in this range the relaxation must be completely dominated by spin diffusion from the amorphous regions, where $T_{1\rho,H}$ is short. The upper limit below which the plot provides a reliable estimate of the motional correlation time is $T_{1\rho,H} < 30$ ms.

The plot of Figure 10 indicates how spin diffusion at long $T_{1\rho,H}$ and the curvature near the $T_{1\rho,H}$ minimum

combine to make the slope of $T_{1\rho,H}(\tau_c)$ smaller than unity. This corresponds to a reduced apparent activation energy in the temperature dependence of $T_{1\rho,H}$; the data shown in Figure 8 give 43 kJ/mol, while the more reliable line shape simulations yield a value of 93 kJ/mol.

**Chain Flips in UHMWPE Fibers.** The $^{13}C$ dipolar line shape and $^1H$ $T_{1\rho}$ data consistently show that the 180° flip rate in the UHMWPE fibers at 360 K is by a factor of 1/20 slower than in HDPE. This slowdown is most likely due to the larger crystallite thickness in the highly crystalline fibers. According to the empirical relation between crystallite thickness and the frequency of the dielectric loss maximum,[20] the crystallite thickness in the UHMWPE fibers is an order of magnitude larger than in the HDPE sample; the crystallite thickness estimated on this basis would be 200 ± 100 nm. The crystal thickness dependence of the motional rate, combined with crystallite thickening at elevated temperature, is probably also the cause for the difference between the motional rate in the HDPE sample before (HDPE-b) and after (HDPE-a) annealing.

In the engineering literature, the α-relaxation is sometimes termed α-transition and the temperature $T_\alpha$ is treated as a transition temperature below which no motion takes place. The continuous temperature dependence of the motional correlation time and the $T_{1\rho,H}$ relaxation time confirm that the motion does not set in abruptly at a specific "transition temperature", as concluded on isotropic samples already a long time ago.[19]

**Comparison with Dynamic-Mechanical and Creep Measurements**. The 180° flips observed directly in this study occur in the crystalline regions. At the same time, they must change the length of the chain segments in the amorphous regions. The chain flips occur between energetically equivalent states of the crystalline part of the chain and therefore do not contribute to the mechanical relaxation. In contrast, the length and associated conformation changes in the amorphous regions can lead to energy dissipation, which results in a mechanical relaxation. This is fully consistent with the earlier observation that the mechanical α-relaxation originates in the amorphous regions but requires the participation of motion in the crystallites.[7]

The excellent mechanical properties of UHMWPE fibers at ambient temperature are due to its high degree of parallel chain orientation and crystallinity, which in turn is a result of its high drawability in the solid state. In ref 6, we present strong evidence that solid-state ultradrawability of polyethylene and other semicrystalline polymers is based on the chain translation associated with the crystalline α-relaxation whose elementary step we have studied here for polyethylenes. The 20-fold slowdown of the flip motion compared to an isotropic sample is the likely origin of gradual strain hardening during the high-temperature draw.[27,50] The significant creep that occurs in UHMWPE fibers at elevated temperatures is a direct manifestation of the α-relaxation. In this regard, the reduction of the motional rate is expected to reduce creep at ambient temperature.

The 20-fold reduction of the chain flip rate in the UHMWPE fibers compared to isotropic HDPE is particularly interesting in view of the observation that the temperature of the maximum mechanical loss modulus E″ or G″ at 1 Hz is similar for both types of materials (60 °C),[32,46,51] as reported specifically by Ward and coworkers.[52] In fact, the flip rate that we have found in the UHMWPE fibers is close to the dynamic-mechanical relaxation rate for ultrahigh-modulus PE fibers obtained from data measured by Ohta et al. (ca. 100 Hz at 360 K).[32] In contrast, in common PE materials the macroscopic mechanical relaxation rates and the microscopic flip rates found by dielectric relaxation or NMR are different by about 2 orders of magnitude; at a temperature around 100 °C the dynamical mechanical relaxation rate is ∼100/s while dielectric and NMR rates are $\sim 10^4$/s.[1,7] The closer agreement of the rates of the two processes in the UHMWPE fibers indicates that in the fibers the 180° chain flip motion is more closely related to the mechanical α-relaxation and creep. The 180° flips occur in the crystallites, while the mechanical α-relaxation is believed to originate in the amorphous regions.[7] Since the chains in UHMWPE fibers are much more extended, it is possible that the two phases are more strongly coupled in their dynamic properties. Ohta et al. also observed that, by incorporating small amounts of $CH_3$ side groups into the main chain, creep of UHMWPE fibers is effectively hindered.[32] This corroborates that the chain flips in the crystallites are indeed closely related to creep.

## 5. Conclusions

The 180° flip motion of chains in the crystallites of $^{13}C-^{13}C$-labeled HDPE was directly confirmed using 2D exchange NMR spectroscopy. The temperature dependence of the motional rate was determined based on 1D line shape changes and stimulated-echo decays. An activation energy of 93 ± 10 kJ/mol was obtained, which is close to that of the dielectric and dynamic-mechanical α-relaxations. A nonexponential correlation function of the motion was observed in the stimulated echo experiments, indicating a width of the relaxation time spectrum of ∼0.5 decades. The relation between the $T_{1\rho,H}$ relaxation time in the crystallites and the correlation time of the 180° flip motion was directly determined. In ultradrawn polyethylene fibers, dipolar satellite narrowing has shown that the crystalline chain segments undergo 180° flips with a reduced rate of ∼150 jumps/s at 360 K. This coincides relatively well with the dynamic-mechanical relaxation rate, indicating a closer relation between the chain flips and creep in the fibers than in isotropic polyethylene where the rates differ by 2 orders of magnitude.

**Acknowledgment.** W.-G.H. and K.S.-R. gratefully acknowledge financial support by the Arnold & Mabel Beckman Foundation and by the National Science Foundation, Grant DMR-9703916. We also thank the late Professor Roger Porter for kindly providing the UHMWPE fibers and for stimulating discussions.

## References and Notes

(1) McCrum, N. G.; Read, B. E.; Williams, G. *Anelastic and Dielectric Effects in Polymeric Solids*; Dover Publications: New York, 1991.
(2) Ward, I. M.; Wilding, M. A. *J. Polym. Sci., Polym. Sci. Ed.* **1984**, *22*, 561−575.
(3) Reneker, D. H. *J. Polym. Sci.* **1962**, *59*, S39−S42.
(4) Strobl, G. *The Physics of Polymers*; Springer-Verlag: Berlin, 1996.
(5) Aharoni, S. M.; Sibilia, J. P. *Polym. Eng. Sci.* **1979**, *19*, 450−455.
(6) Hu, W.-G.; Schmidt-Rohr, K., submitted to *Acta Polymer*.
(7) Boyd, R. H. *Polymer* **1985**, *26*, 323, 1123.

(8) Kentgens, A. P. M.; de Boer, E.; Veeman, W. S. *J. Chem. Phys.* **1987**, *87*, 6859−6866.
(9) Hagemeyer, A.; Schmidt-Rohr, K.; Spiess, H. W. *Adv. Magn. Reson.* **1989**, *13*, 85−130.
(10) Schmidt-Rohr, K.; Spiess, H. W. *Multidimensional Solid-State NMR and Polymers*; Academic Press: New York, 1994.
(11) Schaefer, D.; Spiess, H. W.; Suter, U. W.; Fleming, W. W. *Macromolecules* **1990**, *23*, 3431−3439.
(12) Vega, A. J.; English, A. D. *Macromolecules* **1980**, *13*, 1635−1647.
(13) McCall, D. W.; Douglass, D. C.; Falcone, D. R. *J. Phys. Chem.* **1967**, *71*, 998−1004.
(14) Hirschinger, J.; Schaefer, D.; Spiess, H. W.; Lovinger, A. J. *Macromolecules* **1991**, *24*, 2428−2433.
(15) Schilling, F. C.; Gomez, M. A.; Tonelli, A. E.; Bovey, F. A.; Woodward, A. E. *Macromolecules* **1987**, *20*, 2954−2957.
(16) Beckham, H. W.; Schmidt-Rohr, K.; Spiess, H. W. In *Multidimensional Spectroscopy of Polymers*; Urban, M. W., Provder, T., Eds.; American Chemical Society: Washington, DC, 1995; Vol. 598, pp 243−253.
(17) Olf, H. G.; Peterlin, A. *J. Polym. Sci., Part A-2* **1970**, *8*, 753−797.
(18) Opella, S. J.; Waugh, J. S. *J. Chem. Phys.* **1977**, *66*, 4919−4924.
(19) Hoffman, J. D.; Williams, G.; Passaglia, E. *J. Polym. Sci., Part C* **1966**, *14*, 173−235.
(20) Mansfield, M.; Boyd, R. H. *J. Polym. Sci., Polym. Phys. Ed.* **1978**, *16*, 1227−1252.
(21) Hentschel, D.; Sillescu, H.; Spiess, H. W. *Makromol. Chem.* **1979**, *180*, 241−249.
(22) McCall, D. W.; Douglass, D. C. *Appl. Phys. Lett.* **1965**, *7*, 12−14.
(23) Schmidt-Rohr, K.; Spiess, H. W. *Macromolecules* **1991**, *24*, 5288−5293.
(24) VanderHart, D. L. *J. Magn. Reson.* **1976**, *24*, 467−470.
(25) Boyd, R. H.; Yemni, T. *Polym. Eng. Sci.* **1979**, *19*, 1023−1028.
(26) Hillebrand, L.; Schmidt, A.; Bolz, A.; Hess, M.; Veeman, W. *Macromolecules* **1998**, *31*, 5010−5021.
(27) Porter, R. S.; Wang, L.-H. *J. Macromol. Sci.—Rev. Macromol. Chem. Phys. C* **1995**, *35*, 63−115.
(28) Furuhata, K.; Yokokawa, T.; Seoul, C.; Miyasaka, K. *J. Polym. Sci., Polym. Phys. Ed.* **1986**, *24*, 59−67.
(29) Hu, W.-G.; Schmidt-Rohr, K., submitted to *Polymer*.
(30) Brady, J. M.; Thomas, E. L. *Polymer* **1989**, *30*, 1615−1622.
(31) Ohta, Y.; Sugiyama, H.; Yasuda, H. *J. Polym. Sci., Part B: Polym. Phys.* **1994**, *32*, 261−269.
(32) Ohta, Y.; Yasuda, H. *J. Polym. Sci., Part B: Polym. Phys.* **1994**, *32*, 2241−2249.
(33) Utz, M.; Eisenegger, J.; Suter, U. W.; Ernst, R. R. *J. Magn. Reson.* **1997**, *128*, 217−227.
(34) Schmidt-Rohr, K. *J. Magn. Reson.* **1998**, *131*, 209−217.
(35) Rössler, E. *Chem. Phys. Lett.* **1986**, *128*, 330−334.
(36) Schmidt, C.; Wefing, S.; Blumich, B.; Spiess, H. W. *Chem. Phys. Lett.* **1986**, *130*, 84.
(37) The best fits for 2D exchange (with pure dipolar coupling) and 1D line shape (with both dipolar coupling and chemical shift) yield a C−C bond length of 1.56 ± 0.01 Å and C−C−C bond angle of 112 ± 2°. The bond length result agrees well with neutron scattering data, but the lattice constant $c$ predicted by the simulations is 2.59 ± 0.02 Å, which is bigger than the published value of 2.54 Å from scattering (*Polymer Handbook*, 3rd ed.; Brandrup, J., Immergut, E. H., Eds.; John Wiley & Sons: New York, 1989). The conflict is even more remarkable if the satellite positions in the UHMWPE fiber spectrum are applied to calculate the $c$ value. Our best fit for $R_1$ and $R_2$ peak positions (1740 and 620 Hz, respectively, which agree with experimental values within the error limit) yields a bond length of 1.56 ± 0.01 Å and a bond angle of 116 ± 2°. The $R_2$ peak position of 620 Hz directly gives a lattice constant $c$ of 2.65 ± 0.02 Å, much higher than the published value from scattering measurements. This agrees with the NMR results of VanderHart (VanderHart, D. L. *J. Magn. Reson.* **1976**, *24*, 467−470), who noticed that the position of $R_2$, 600 Hz from the center, deviates from the value of 700 Hz calculated based on the dipolar coupling strength with $c = 2.54$ Å from X-ray scattering. He considered many potential reasons for the reduction of the coupling, but the deviation was not fully explained. Our experiment was performed at a much higher $B_0$ field strength and nevertheless found that the $R_2$ position remains the same (590 Hz). This shows that the deviation is intrinsic and not related to the magnetic field strength.
(38) Abragam, A. *Principles of Nuclear Magnetism*; Oxford University Press: Oxford, 1961.
(39) VanderHart, D. L. *J. Chem. Phys.* **1976**, *64*, 830−834.
(40) Tzou, D. L.; Schmidt-Rohr, K.; Spiess, H. W. *Polymer* **1994**, *35*, 4728−4733.
(41) Johansson, A.; Wendsjö, A.; Tegenfeldt, J. *Electrochim. Acta* **1992**, *37*, 1487−1489.
(42) Packer, K. J.; Pope, J. M.; Yeung, R. R.; Cudby, M. E. A. *J. Polym. Sci., Polym. Phys. Ed.* **1984**, *22*, 589−616.
(43) Noid, D. W.; Sumpter, B. G.; Wunderlich, B. *Macromolecules* **1991**, *24*, 4148−4151.
(44) Lindsey, C. P.; Patterson, G. D. *J. Chem. Phys.* **1980**, *73*, 3348−3357.
(45) Ashcraft, C. R.; Boyd, R. H. *J. Polym. Sci., Polym. Phys. Ed.* **1976**, *14*, 2153−2193.
(46) Boyd, R. H. *Macromolecules* **1984**, *17*, 903−911.
(47) Reddish, W.; Barrie, J. T. *I. U. P. A. C. Symp. über Macromol*, Wiesbaden, Kurzmitteilung I.A.3, 1959.
(48) Kuwabara, K.; Kaji, H.; Horii, F.; Bassett, D. C.; Olley, R. H. *Macromolecules* **1997**, *30*, 7516−7521.
(49) Syi, J.-L.; Mansfield, M. L. *Polymer* **1988**, *29*, 987−997.
(50) Lemstra, P. J.; Kirschbaum, R.; Ohta, T.; Yasuda, H. In *Developments in Oriented Polymers-2*; Ward, I. M., Ed.; Elsevier Applied Science: London, 1987; pp 39−77.
(51) In this comparison, we refer to literature data on other UHMWPE fiber samples; this is permissible because the chain flip rate is relatively insensitive to the crystallite thickness (Mansfield, M.; Boyd, R. H. *J. Polym. Sci., Polym. Phys. Ed.* **1978**, *16*, 1227−1252) in the 100 nm range that is relevant for UHMWPE fibers (Hu, W.-G.; Schmidt-Rohr, K., submitted to *Polymer*).
(52) Gibson, A. G.; Davies, G. R.; Ward, I. M. *Polymer* **1978**, *19*, 683−693.

MA981138T